

Notice of Copyright This manuscript has been authored by UT-Battelle, LLC under Contract No. DE-AC05-00OR22725 with the U.S. Department of Energy. The United States Government retains and the publisher, by accepting the article for publication, acknowledges that the United States Government retains a non-exclusive, paid-up, irrevocable, world-wide license to publish or reproduce the published form of this manuscript, or allow others to do so, for United States Government purposes. The Department of Energy will provide public access to these results of federally sponsored research in accordance with the DOE Public Access Plan (<http://energy.gov/downloads/doe-public-access-plan>).

High Phonon Scattering Rates Suppress Thermal Conductivity in Hyperstoichiometric Uranium Dioxide

Hao Ma,^{1*} Matthew S. Bryan,¹ Judy W. L. Pang,¹ Douglas L. Abernathy,² Daniel J. Antonio,³ Krzysztof Gofryk,³ and Michael E. Manley^{1*}

¹*Materials Science and Technology Division, Oak Ridge National Laboratory, Oak Ridge, Tennessee 37831, USA*

²*Neutron Scattering Division, Oak Ridge National Laboratory, Oak Ridge, Tennessee 37831, USA*

³*Idaho National Laboratory, Idaho Falls, Idaho 83415, USA*

Abstract

Uranium dioxide (UO₂), one of the most important nuclear fuels, can accumulate excess oxygen atoms as interstitial defects, which significantly impacts thermal properties. In this study, thermal conductivities and inelastic neutron scattering measurements on UO₂ and UO_{2+x} (x=0.3, 0.4, 0.8, 0.11) were performed at low temperatures (2-300 K). The thermal conductivity of UO_{2+x} is significantly suppressed compared to UO₂ except near the Néel temperature $T_N=30.8$ K, where it is independent of x . Phonon measurements demonstrate that the heat capacities and phonon group velocities of UO₂ and UO_{2+x} are similar and that the suppressed thermal conductivity in UO_{2+x} results from high phonon scattering rates. These new insights advance our fundamental understanding of thermal transport properties in advanced nuclear fuels.

Keywords

Hyperstoichiometric uranium dioxide, Thermal conductivity, Inelastic neutron scattering, Phonon density of states, High phonon scattering rates

* Corresponding author. Email: mah1@ornl.edu

* Corresponding author. Email: manley@ornl.gov

1. Introduction

Uranium dioxide is the most widely used nuclear fuel and its thermal properties are important to reactor safety and performance[1]. UO_2 is able to accommodate a variable stoichiometry, depending on temperature and oxygen pressure[2, 3]. For example, UO_2 can be oxidized by water vapor in the rare event of a cladding breach in a reactor, which consequently raises ratio of oxygen to uranium ($\text{O/U}=2+x$)[2]. The excess oxygen atoms in hyperstoichiometric uranium dioxide ($x > 0$) were identified as interstitial defects that form partially ordered clusters[4-6]. In addition, the O/U ratio is one of the most important parameters governing fuel safety because it significantly affects the thermal properties such as the melting point[7] and thermal conductivity[8-12]. For example, Manara *et al.*[7] found the melting point of UO_{2+x} ($x = 0-0.21$) decreases as the O/U ratio increases. White *et al.*[11] reported that UO_{2+x} pellets exhibit a decrease in thermal conductivity with increasing temperature and follow $1/T$ dependence due to the anharmonic Umklapp phonon-phonon scattering at 363 -1673 K. The thermal conductivity of UO_{2+x} also decreases as x increases, indicating the importance of phonon-defects scattering.

Although there are many studies of the thermal properties of UO_{2+x} at high temperatures (300-1700 K)[7-13], there is little information on the thermal conductivity and phonon properties of UO_{2+x} at low temperatures (below 300 K). The effects of excess oxygen atoms (x) on the thermal conductivity of UO_{2+x} at low temperatures, especially around Néel temperature $T_N = 30.8$ K, are of critical importance in bench marking theoretical models. In this study, the thermal conductivity of UO_2 and UO_{2+x} single crystals are reported in the temperature range of 2-300 K. We find that UO_{2+x} has a much smaller thermal conductivity than UO_2 at all temperatures except near the Néel temperature, where it is unaffected. The phonon density of states (PDOS) and scattering function measured by inelastic neutron scattering (INS) demonstrate that the suppressed thermal conductivity in UO_{2+x} originates with an increased phonon scattering rate with the addition of oxygen interstitial defects.

2. Method

2.1 Samples preparation and thermal conductivity measurements

Thermal conductivity measurements were performed in a DynaCool-9 Quantum Design Measurement System. The measurements were performed in the continuous heating mode of the TTO option using a pulse-power steady-state method. The crystals were measured from 2 to 300 K at 0.25 K/min. The oxygen stoichiometry of the UO_2 single crystals was set in a thermogravimetric analyzer by controlling the oxygen activity and by adjusting the partial pressure of oxygen at 1273 K. Then, the final stoichiometry of the UO_{2+x} crystals was calculated from the sample weight change relative to the stoichiometric UO_2 reference data. The size of these crystals is around $1 \times 1 \times 3 \text{ mm}^3$.

2.2. INS measurements

The single crystals used in the thermal conductivity measurements are too small for direct INS measurement on phonon dispersion and especially phonon linewidths. Hence, to characterize the phonon properties, instead INS measurements on powders of UO_2 and $\text{UO}_{2.08}$ at 77 K and 295 K were performed using the wide Angular Range Chopper Spectrometer (ARCS) at the Spallation

Neutron Source (SNS) of Oak Ridge National Laboratory[14]. The setup of the spectrometer was identical to previously reported PDOS measurements for UO_2 [15, 16]. An incident neutron energy of $E_i=120$ meV was used, which is high enough to capture the phonon cutoff around 80 meV and allows for summing over enough zones in momentum space to obtain a PDOS. Scattering introduced by the sample can and the cryostat were corrected for by subtracting the corresponding spectra from a duplicate, empty sample can measurement. The corrected scattered neutron intensities, $I(\Phi, t)$, were converted to the scattering function $S(Q, E)$, where Q is momentum transfer magnitude and E is the energy transfer. Other experimental details can be found elsewhere[15, 16] and are not repeated here. The neutron weighted PDOS $g^{NW}(E)$ was then obtained by integrating $S(Q, E)$ over Q values ranging from 4 to 10 \AA^{-1} for both UO_2 and $\text{UO}_{2.08}$, and then correcting for multiphonon scattering (using iterative procedure), the Debye-Waller factor, thermal population factor, and subtracting the elastic peak.

The measured neutron weighted PDOS can be expressed as

$$g^{NW}(E) = \frac{\sigma_U}{M_U} g_U(E) + 2 \frac{\sigma_O}{M_O} g_O(E) \quad (1)$$

where g_i , M_i and σ_i are the partial PDOS, the atomic mass, and the corresponding neutron scattering cross section of element i ($i = \text{U}$ or O).[15, 17] In order to extract the neutron unweighted PDOS, we take advantage of the fact that nearly all phonon modes below 25 meV are from uranium and nearly all phonon modes above 25 meV are from oxygen[15, 18, 19].

The specific heat at constant pressure, C_P , can be written

$$C_P - C_V = 9\alpha^2 B v T \quad (2)$$

where C_V is the specific heat at constant volume, α is the linear thermal expansion, B is bulk modulus, v is molar volume, and T is temperature[20]. The phonon contribution to the specific heat at constant volume C_V^{ph} can be obtained directly from the neutron unweighted PDOS using:

$$C_V^{ph}(T) = 3k_B \int_0^\infty g_{T_0} \frac{E^2}{(k_B T)^2} \frac{e^{\frac{E}{k_B T}}}{(e^{\frac{E}{k_B T}} - 1)^2} dE \quad (3)$$

where k_B and $g_{T_0}(E)$ are the Boltzmann constant and neutron unweighted PDOS at temperature T_0 , respectively[16].

3. Results and discussion

The measured thermal conductivity of UO_{2+x} single crystals as a function of temperature is shown in Fig. 1a. The thermal conductivity of UO_{2+x} for all values of x measured exhibits a double-peak behavior where maxima occur at ~ 10 and 220 K and a minimum occurs at the Néel temperature $T_N = 30.8$ K, consistent with previous studies on UO_2 [21-23]. In addition, other than in the vicinity of T_N , the thermal conductivity of UO_{2+x} is significantly suppressed compared to UO_2 and decreases with increasing x (see Fig. 1b). The decreasing thermal conductivity with increasing x is likely driven by phonon-defects scattering and is similar to the observed high temperature behavior[8-12]. More specifically, the thermal conductivity of $\text{UO}_{2.08}$ (2.68 W/(mK)) is 67% the value for UO_2 at 77 K (4.46 W/(mK)). Interestingly, the thermal conductivity of UO_{2+x} (~ 1 W/(mK)) is essentially

independent of the x at $T_N = 30.8$ K, indicating negligible phonon-defects scattering likely due to strong magnetic fluctuations, see Fig. 1b.

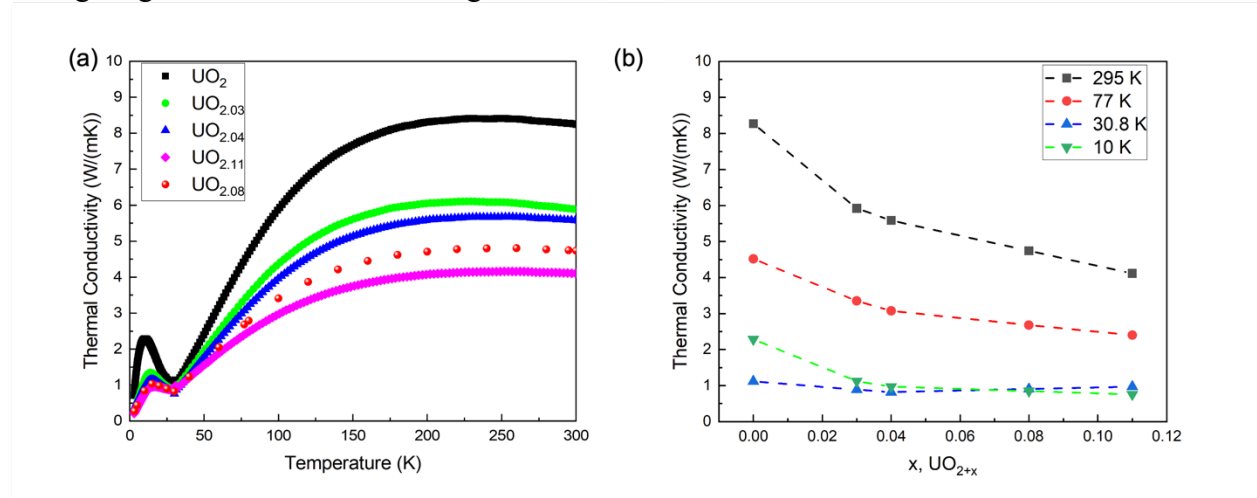


Fig. 1. (a) Measured thermal conductivity of UO_2 and UO_{2+x} single crystals as a function of temperature. Thermal conductivity of $\text{UO}_{2.08}$ is obtained by interpolation between $\text{UO}_{2.04}$ and $\text{UO}_{2.11}$ (b) Measured thermal conductivity of UO_{2+x} single crystals as a function of the excess oxygen atoms x at several different temperatures.

To gain deeper insights on the suppressed thermal conductivity in UO_{2+x} , we first checked the structure of $\text{UO}_{2.08}$ and the measured neutron diffraction pattern of $\text{UO}_{2.08}$ in Fig. S1 of Supplementary Materials (SM) shows that $\text{UO}_{2.08}$ adopts a superlattice structure which is a mix of UO_2 and U_4O_9 , consistent with reported phase diagram at low temperatures[13, 24, 25]. We then measured their neutron weighted PDOS of UO_2 and $\text{UO}_{2.08}$ at 77 K and 295 K, as shown in Fig. 2a and 2b. Well-defined zone-boundary phonon peaks are observed at energies of 12, 21, 33, 56, and 72 meV for both UO_2 and $\text{UO}_{2.08}$ at 77 K and 295 K. With reference to the phonon dispersion of UO_2 [15, 17], the uranium-dominated transverse acoustic (TA) and the longitudinal acoustic (LA) zone-boundary phonon energies correspond to the 12 and 21 meV peaks. These peaks show trivial difference between UO_2 and $\text{UO}_{2.08}$. The oxygen-dominated transverse optical (TO1 and TO2) and the longitudinal optical LO2 zone-boundary phonon energies correspond to the remaining 33, 56, and 72 meV peaks, respectively. In contrast, these peaks in $\text{UO}_{2.08}$ are less intense and slightly broader than that in UO_2 . In addition, there are some nonnegligible intensities above phonon cutoff (78meV), which is consistent with nonlinear propagating modes (NPM) identified in a previous study[26].

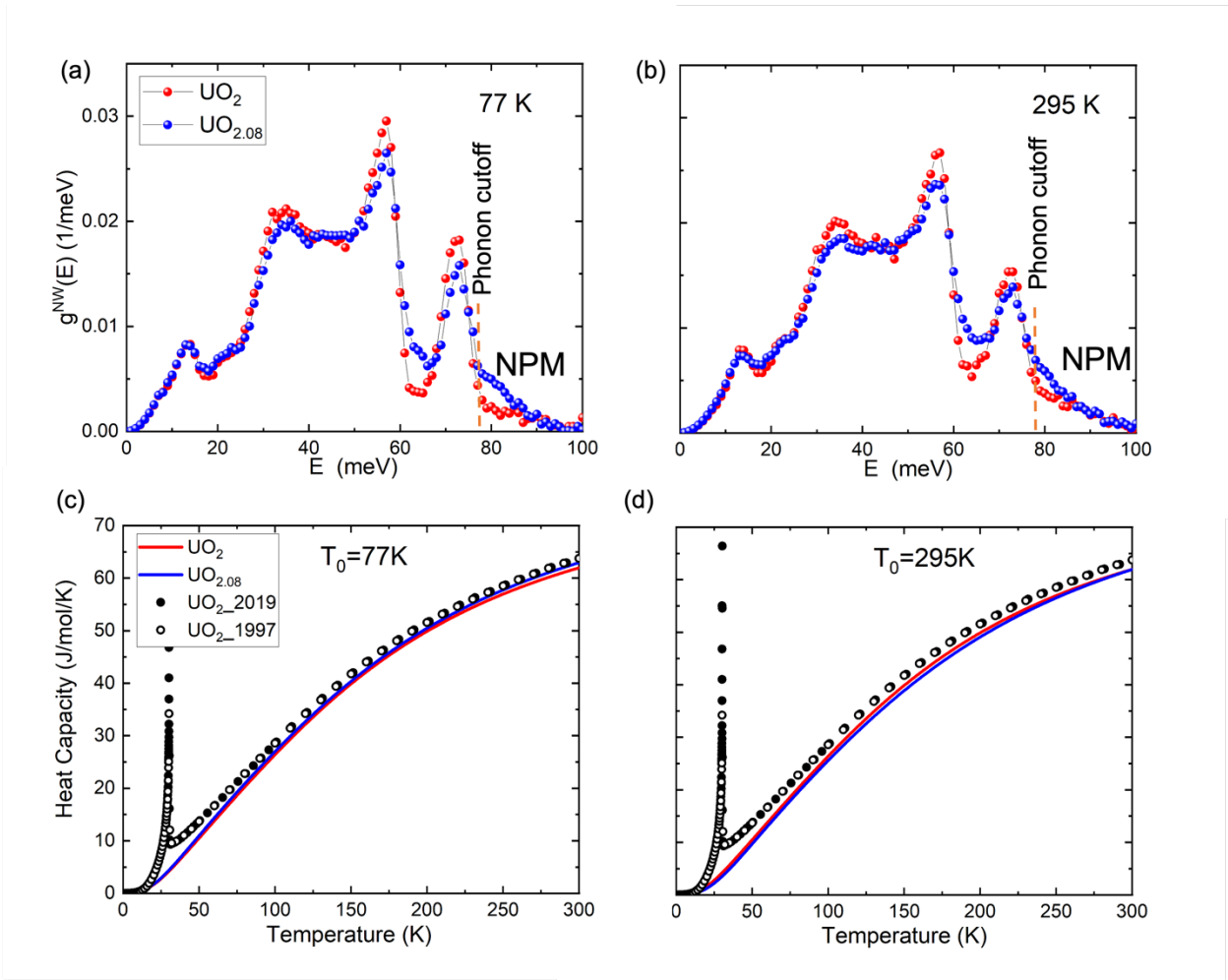


Fig. 2. The neutron weighted PDOS of UO_2 (red spheres) and $UO_{2.08}$ (blue spheres) powders measured by INS at (a) 77 K (b) 295 K; The specific heat capacity (C_P) of UO_2 (red line) and $UO_{2.08}$ (blue line) with respect to temperature were calculated using unweighted PDOS at (c) $T_0 = 77$ K and (d) $T_0 = 295$ K. Solid and open black circles are previous experimental C_P of UO_2 single crystal[16] and sintered powder[27]. A sharp spike at $T_N = 30.8$ K is a result of the Néel transition from an antiferromagnetic state to a paramagnetic state.

The calculated specific heat capacities (C_P) of UO_2 and $UO_{2.08}$ using the neutron unweighted 77K and 295K- PDOS based on equation (2) and (3) are shown in Fig. 2c and 2d. Our calculated C_P of UO_2 shows good agreement with the experimental C_P [16, 27], except in the vicinity of T_N where magnetic contributions are large[28-30]. Moreover, C_P of UO_2 and $UO_{2.08}$ are almost the same (less than 2% difference) over the entire temperature range of 2-300 K. Note that their C_V^{ph} also show trivial difference as shown in Fig. S2 of SM.

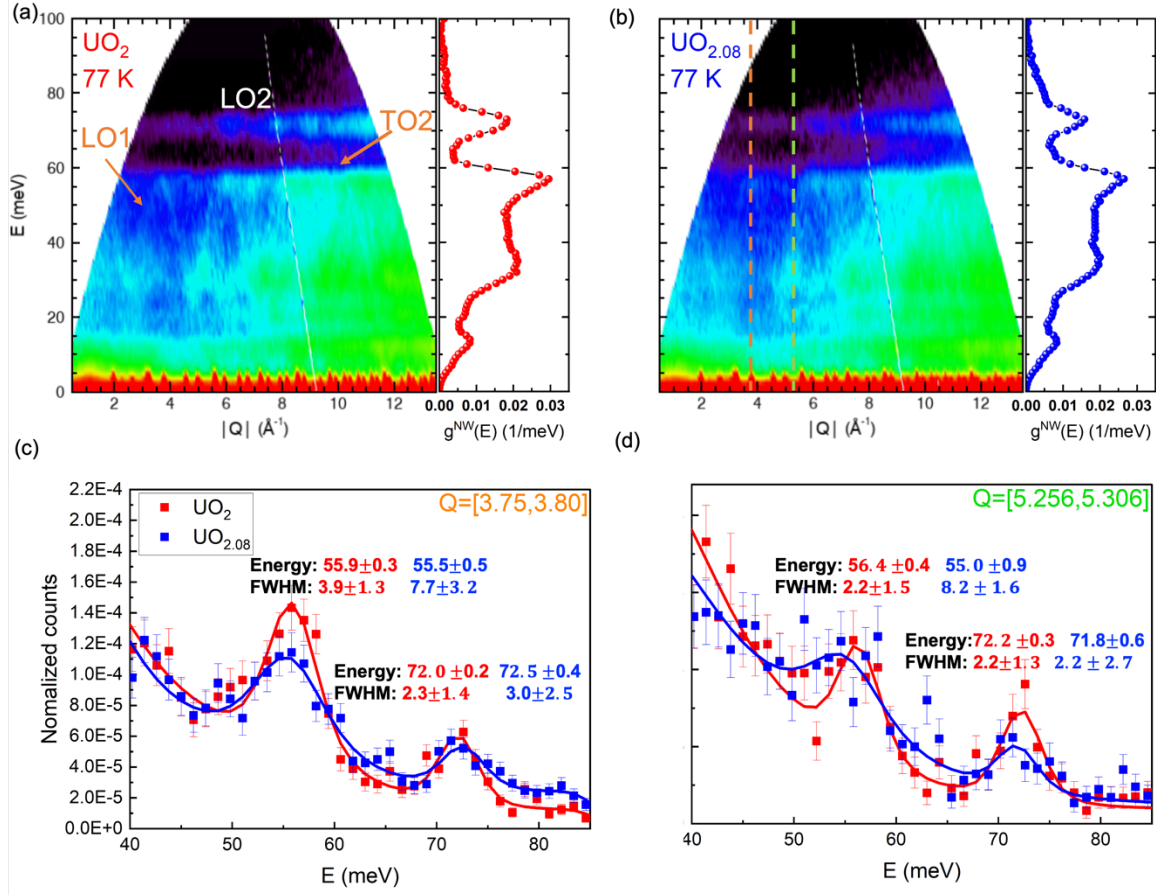


Fig. 3. Color contour plots of the scattering function $S(Q,E)$ as a function of E and Q and their corresponding neutron-weighted PDOS for (a) UO_2 and (b) $\text{UO}_{2.08}$ powders at 77K measured by INS. Scattering function as a function of energy at (c) $Q=[3.75,3.8]$ and (d) $Q=[5.256,5.306]$, corresponding to orange and blue dashed lines in the color contour plot (b). Red and blue lines in (c) and (d) are theoretical fittings of these INS data. Fitted phonon energies and linewidths are shown in the insert. Red and blue denote UO_2 and $\text{UO}_{2.08}$, respectively.

Thermal conductivity (k) of single crystals in the phonon gas model is quantitatively defined by

$$k = 1/3 C_V^{ph} V_g \tau^2 \quad (4)$$

where C_V^{ph} , V_g , and τ are the phonon heat capacity, the average phonon group velocity, and the average phonon lifetimes, respectively. With the similar C_V^{ph} and V_g in UO_2 and $\text{UO}_{2.08}$, the lower thermal conductivity in $\text{UO}_{2.08}$ must result from smaller average phonon lifetimes, i.e. higher phonon scattering rates than UO_2 . For example, given that the thermal conductivity of $\text{UO}_{2.08}$ is 67% the value of UO_2 at 77 K, the average phonon lifetimes in $\text{UO}_{2.08}$ are 82% the value of UO_2 . To validate this, we plot the measured scattering function $S(Q,E)$ as a function of E and Q at 77 K in Fig. 3a and 3b. ($S(Q,E)$ at 295 K can be found in Fig. S3 of SM). Interestingly, both $S(Q,E)$ contour plots exhibit clear sinusoidal shapes at the energy range of 20-55 meV and flat shapes at 56 meV and 72 meV, corresponding to LO1, TO2 and LO2 phonon branches along [100] direction. Moreover, LO1 phonon branches in $\text{UO}_{2.08}$ are broader than UO_2 , which represents larger linewidths or higher phonon scattering rates in $\text{UO}_{2.08}$. Note that the LO1 phonon branches were found to contribute to the largest amount (>30%) of total thermal conductivity in UO_2 . [17] Further

energy cuts at $Q=[3.75,3.8]$ and $Q=[5.256,5.306]$ are shown in Fig. 3c and 3d. The fitted phonon energies of TO2 and LO2 modes in UO_2 are very close to $UO_{2.08}$, which reiterates the similar group velocities in them. The fitted phonon linewidths of TO2 and LO2 modes in UO_2 are 3.9 ± 1.3 meV and 2.3 ± 1.4 meV at $Q=[3.75,3.8]$, and 2.2 ± 1.5 meV and 2.2 ± 2.7 meV at $Q=[5.256,5.306]$, comparable to previously measured linewidths (2-3 meV) in UO_2 single crystal¹⁷. The phonon lifetimes (inverse of linewidths) of TO2 in $UO_{2.08}$ are 0.52 ps at $Q=[3.75,3.8]$ and 0.50 ps at $Q=[5.256,5.306]$, which are 49% of 1.06 ps and 27% of 1.88 ps in UO_2 . In contrast, phonon lifetimes of LO2 in $UO_{2.08}$ are 1.80 ps at $Q=[3.75,3.8]$ and 1.88 ps at $Q=[5.256,5.306]$, which are almost the same as the corresponding values in UO_2 (1.38 ps at $Q=[3.75,3.8]$ and 1.88 ps at $Q=[5.256,5.306]$). In brief, with similar C_V^{ph} and V_g in UO_2 and UO_{2+x} , small phonon lifetimes, i.e. high phonon scattering rates, lead to much lower thermal conductivity in UO_{2+x} .

4. Conclusion

In summary, we performed thermal conductivity and INS measurements on UO_2 and UO_{2+x} at low temperatures (2-300 K). It is found that the thermal conductivities of all UO_{2+x} single crystals exhibit a double-peak behavior where maxima occur at 10 and 220 K and a minimum occurs at the Néel temperature $T_N=30.8$ K, consistent with previous studies on UO_2 . Except in the vicinity of T_N , the thermal conductivity of UO_{2+x} is significantly suppressed compared to UO_2 and decreases with the increasing of x . At $T_N=30.8$ K, the thermal conductivity of UO_{2+x} is essentially independent of the x . Further INS measurements of the PDOS and scattering function demonstrate that heat capacity and phonon group velocities of UO_2 and UO_{2+x} are similar and thus the suppressed thermal conductivity is attributed to high phonon scattering rates in UO_{2+x} . The fundamental new knowledge gained from this study may guide the future design of safe and efficient nuclear reactors.

Acknowledgement

H. M., M.S.B., K.G. and M.E.M. were supported by the Center for Thermal Energy Transport under Irradiation, an Energy Frontier Research Center funded by the U.S. Department of Energy (DOE), Office of Science, United States, Office of Basic Energy Sciences. D.J.A. and K.G. acknowledge support from Advanced Fuel Campaign program (INL). Portions of this research used resources at the Spallation Neutron Source, a U.S. DOE Office of Science User Facility operated by the Oak Ridge National Laboratory. We are grateful to David A. Andersson and Christopher R. Stanek for providing UO_{2+x} crystals for the thermal conductivity measurements.

The data that supports the findings of this study are available within the article and its supplementary material.

Reference

- [1] D.H. Hurley, A. El-Azab, M.S. Bryan, M.W.D. Cooper, C.A. Dennett, K. Gofryk, L. He, M. Khafizov, G.H. Lander, M.E. Manley, J.M. Mann, C.A. Marianetti, K. Rickert, F.A. Selim, M.R. Tonks, J.P. Wharry, Thermal Energy Transport in Oxide Nuclear Fuel, Chemical Reviews, DOI 10.1021/acs.chemrev.1c00262(2021).
- [2] W.T. Thompson, B.J. Lewis, E.C. Corcoran, M.H. Kaye, S.J. White, F. Akbari, Z. He, R. Verrall, J.D. Higgs, D.M. Thompson, T.M. Besmann, S.C. Vogel, Thermodynamic treatment of uranium dioxide based nuclear fuel, International Journal of Materials Research, 98 (2007) 1004-1011.

- [3] D.R. Olander, Mechanistic interpretations of UO₂ oxidation, *Journal of Nuclear Materials*, 252 (1998) 121-130.
- [4] J. Wang, R.C. Ewing, U. Becker, Average structure and local configuration of excess oxygen in UO_{2+x}, *Scientific Reports*, 4 (2014) 4216.
- [5] B.T.M. Willis, Positions of the Oxygen Atoms in UO_{2.13}, *Nature*, 197 (1963) 755-756.
- [6] B. Willis, The defect structure of hyper-stoichiometric uranium dioxide, *Acta Crystallographica Section A: Crystal Physics, Diffraction, Theoretical and General Crystallography*, 34 (1978) 88-90.
- [7] D. Manara, C. Ronchi, M. Sheindlin, M. Lewis, M. Brykin, Melting of stoichiometric and hyperstoichiometric uranium dioxide, *Journal of Nuclear Materials*, 342 (2005) 148-163.
- [8] F.J. Hetzler, E.L. Zebroski, THERMAL CONDUCTIVITY OF STOICHIOMETRIC AND HYPOSTOICHIOMETRIC URANIUM OXIDE AT HIGH TEMPERATURES, *Transactions of the American Nuclear Society*, DOI (1964).
- [9] L.A. Goldsmith, J.A.M. Douglas, Measurements of the thermal conductivity of uranium dioxide at 670 1270 K, *Journal of Nuclear Materials*, 47 (1973) 31-42.
- [10] M. Amaya, T. Kubo, Y. Korei, Thermal Conductivity Measurements on UO_{2+x} from 300 to 1,400 K, *Journal of Nuclear Science and Technology*, 33 (1996) 636-640.
- [11] J.T. White, A.T. Nelson, Thermal conductivity of UO_{2+x} and U₄O_{9-y}, *Journal of Nuclear Materials*, 443 (2013) 342-350.
- [12] S. Yamasaki, T. Arima, K. Idemitsu, Y. Inagaki, Evaluation of Thermal Conductivity of Hyperstoichiometric UO_{2+x} by Molecular Dynamics Simulation, *International Journal of Thermophysics*, 28 (2007) 661-673.
- [13] X.Y. Liu, M.W.D. Cooper, K.J. McClellan, J.C. Lashley, D.D. Byler, B.D.C. Bell, R.W. Grimes, C.R. Stanek, D.A. Andersson, Molecular Dynamics Simulation of Thermal Transport in UO_2 Containing Uranium, Oxygen, and Fission-product Defects, *Physical Review Applied*, 6 (2016) 044015.
- [14] D.L. Abernathy, M.B. Stone, M.J. Loguillo, M.S. Lucas, O. Delaire, X. Tang, J.Y.Y. Lin, B. Fultz, Design and operation of the wide angular-range chopper spectrometer ARCS at the Spallation Neutron Source, *Review of Scientific Instruments*, 83 (2012) 015114.
- [15] J.W.L. Pang, A. Chernatynskiy, B.C. Larson, W.J.L. Buyers, D.L. Abernathy, K.J. McClellan, S.R. Phillpot, Phonon density of states and anharmonicity of UO_2 , *Physical Review B*, 89 (2014) 115132.
- [16] M.S. Bryan, J.W.L. Pang, B.C. Larson, A. Chernatynskiy, D.L. Abernathy, K. Gofryk, M.E. Manley, Impact of anharmonicity on the vibrational entropy and specific heat of UO_2 , *Physical Review Materials*, 3 (2019) 065405.
- [17] J.W.L. Pang, W.J.L. Buyers, A. Chernatynskiy, M.D. Lumsden, B.C. Larson, S.R. Phillpot, Phonon Lifetime Investigation of Anharmonicity and Thermal Conductivity of UO_2 by Neutron Scattering and Theory, *Physical Review Letters*, 110 (2013) 157401.
- [18] T. Arima, S. Yamasaki, Y. Inagaki, K. Idemitsu, Evaluation of thermal properties of UO₂ and PuO₂ by equilibrium molecular dynamics simulations from 300 to 2000K, *Journal of Alloys and Compounds*, 400 (2005) 43-50.
- [19] P. Goel, N. Choudhury, S.L. Chaplot, Fast ion diffusion, superionic conductivity and phase transitions of the nuclear materials UO₂ and Li₂O, *Journal of Physics: Condensed Matter*, 19 (2007) 386239.
- [20] D.C. Wallace, *Statistical Physics of Crystals and Liquids*.

- [21] K. Gofryk, S. Du, C.R. Stanek, J.C. Lashley, X.Y. Liu, R.K. Schulze, J.L. Smith, D.J. Safarik, D.D. Byler, K.J. McClellan, B.P. Uberuaga, B.L. Scott, D.A. Andersson, Anisotropic thermal conductivity in uranium dioxide, *Nature Communications*, 5 (2014) 4551.
- [22] J.P. MOORE, D.L. MCELROY, Thermal Conductivity of Nearly Stoichiometric Single-Crystal and Polycrystalline UO_2 , *Journal of the American Ceramic Society*, 54 (1971) 40-46.
- [23] K. Shrestha, T. Yao, J. Lian, D. Antonio, M. Sessim, M.R. Tonks, K. Gofryk, The grain-size effect on thermal conductivity of uranium dioxide, *Journal of Applied Physics*, 126 (2019) 125116.
- [24] J.D. Higgs, W.T. Thompson, B.J. Lewis, S.C. Vogel, Kinetics of precipitation of U_4O_9 from hyperstoichiometric UO_{2+x} , *Journal of Nuclear Materials*, 366 (2007) 297-305.
- [25] R.I. Palomares, M.T. McDonnell, L. Yang, T. Yao, J.E.S. Szymanowski, J. Neufeind, G.E. Sigmon, J. Lian, M.G. Tucker, B.D. Wirth, M. Lang, Oxygen point defect accumulation in single-phase $\text{U}\{\text{O}\}_{2+x}$, *Physical Review Materials*, 3 (2019) 053611.
- [26] M.S. Bryan, L. Fu, K. Rickert, D. Turner, T.A. Prusnick, J.M. Mann, D.L. Abernathy, C.A. Marianetti, M.E. Manley, Nonlinear propagating modes beyond the phonons in fluorite-structured crystals, *Communications Physics*, 3 (2020) 217.
- [27] J.J. Huntzicker, E.F. Westrum, The magnetic transition, heat capacity, and thermodynamic properties of uranium dioxide from 5 to 350 K, *The Journal of Chemical Thermodynamics*, 3 (1971) 61-76.
- [28] G.D. Khattak, Specific heat of uranium dioxide (UO_2) between 0.3 and 50 K, *physica status solidi (a)*, 75 (1983) 317-321.
- [29] R. De Batist, R. Gevers, M. Verschueren, Magnon Contribution to the Low-Temperature Specific Heat of UO_2 , *physica status solidi (b)*, 19 (1967) 77-88.
- [30] A.P. Cracknell, S.J. Joshua, The Spin-Wave Dispersion Relations and the Spin-Wave Contribution to the Specific Heat of Antiferromagnetic UO_2 , *physica status solidi (b)*, 36 (1969) 737-745.

Supplementary Materials

High Phonon Scattering Rates Suppress Thermal Conductivity in Hyperstoichiometric Uranium Dioxide

Hao Ma,^{1*} Matthew S. Bryan,¹ Judy W. L. Pang,¹ Douglas L. Abernathy,² Daniel J. Antonio,³ Krzysztof Gofryk,³ and Michael E. Manley^{1*}

¹*Materials Science and Technology Division, Oak Ridge National Laboratory, Oak Ridge, Tennessee 37831, USA*

²*Neutron Scattering Division, Oak Ridge National Laboratory, Oak Ridge, Tennessee 37831, USA*

³*Idaho National Laboratory, Idaho Falls, Idaho 83415, USA*

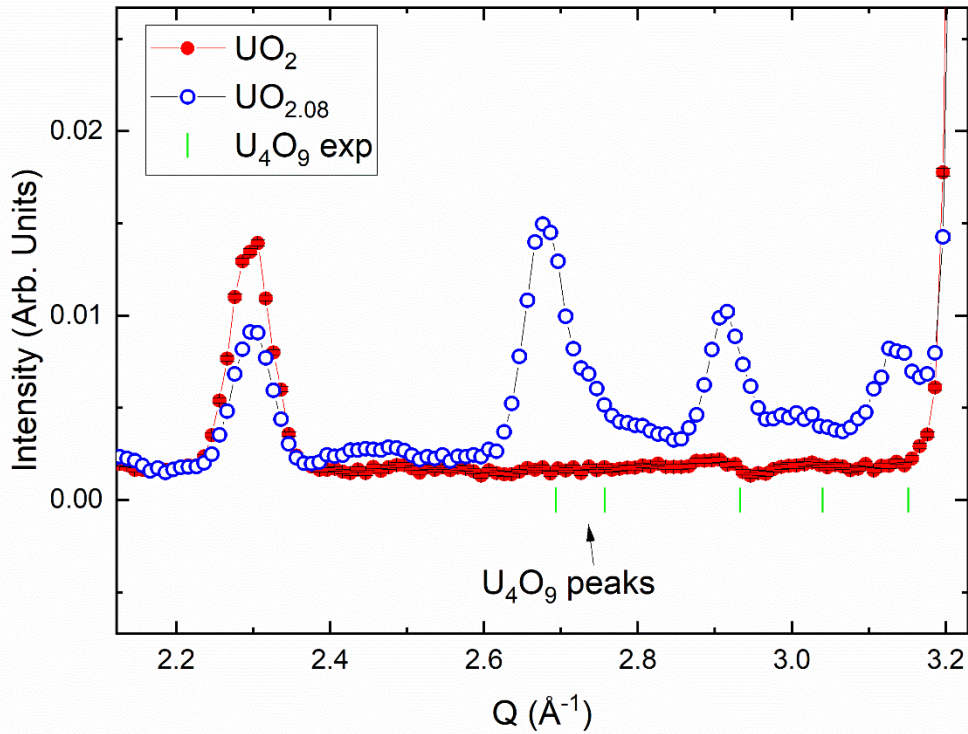


Fig. S1. The measured neutron diffraction patterns of UO_2 and $\text{UO}_{2.08}$ at 295 K. U_4O_9 data is from Ref. 1.

* Corresponding author. Email: mah1@ornl.edu

* Corresponding author. Email: manley@ornl.gov

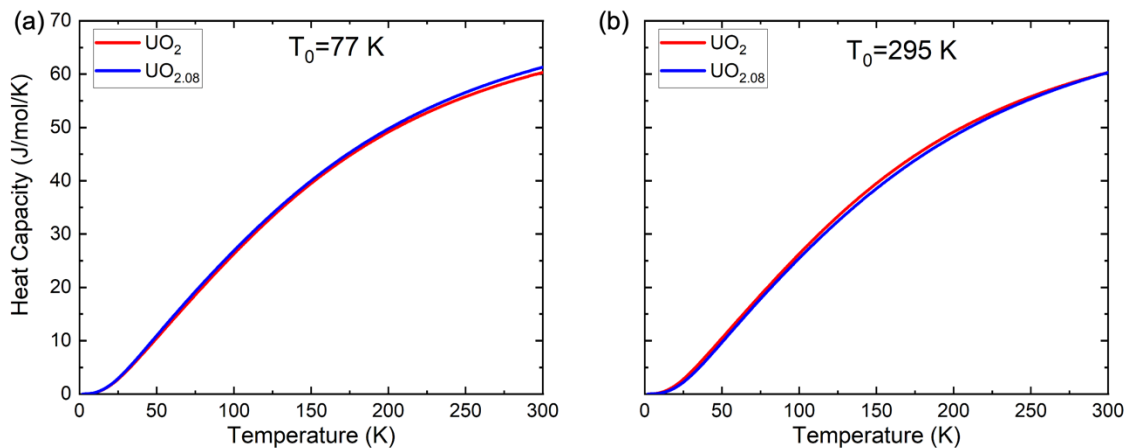


Fig. S2. The heat capacity (C_V^{ph}) of UO_2 (red line) and $\text{UO}_{2.08}$ (blue line) with respect to temperature were calculated using unweighted PDOS at (c) $T_0=77 \text{ K}$ and (d) $T_0=295 \text{ K}$.

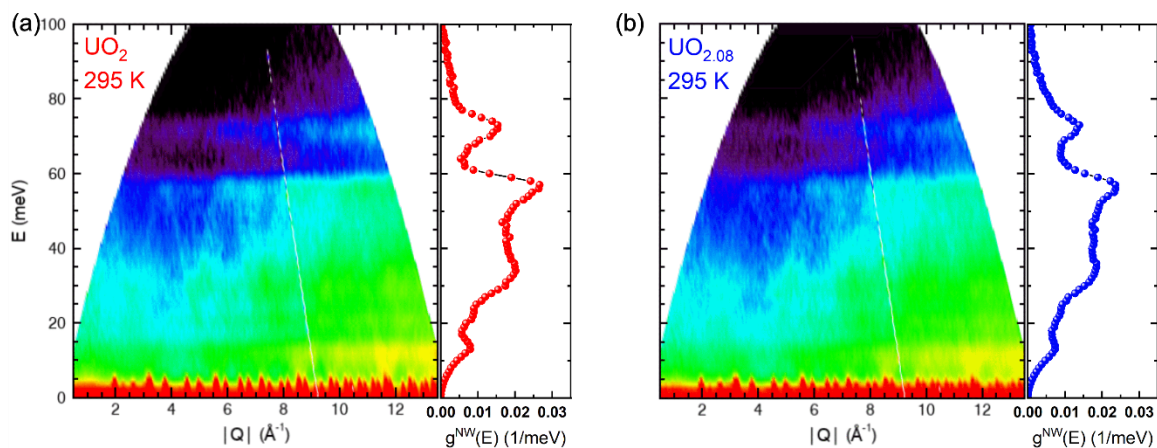


Fig. S3. Color contour plots of the scattering function $S(Q, E)$ as a function of E and Q and their corresponding neutron-weighted PDOS for (a) UO_2 and (b) $\text{UO}_{2.08}$ at 295 K measured by INS.

References

1. Garrido, F., *et al.*, *Inorganic Chemistry* (2006) **45** (20), 8408